The endogenous metabolite hypochlorite activates indoleamine 2,3-dioxygenase-1 for catalysis: Functional and mechanistic implications

Setareh Saryazdi and Steven G. Van Lanen*

Department of Pharmaceutical Sciences, College of Pharmacy, University of Kentucky, Lexington, Kentucky 40536, USA.

*Correspondence and requests for materials should be addressed to S.V.L. (email: svanlanen@uky.edu)

Keywords: L-tryptophan, L-kynurenine, metabolism, immunology, hypochlorous acid, reactive oxygen species

Abstract

Indolamine 2,3-dioxygenase (IDO1) is a hemoprotein that catalyzes the oxidative cleavage of L-tryptophan (L-Trp) to *N′*-formyl-L-kynurenine (L-NFK) along the kynurenine pathway. Its activity depletes L-Trp while initiating a signaling cascade culminating in an immunosuppressive outcome of clinical significance. The generally used in vitro activity assay for IDO1 relies on ascorbic acid and synthetic methylene blue, with the endogenous activator still uncertain. Here we demonstrate sodium hypochlorite, commonly known as bleach, functions as an in vitro activator/cofactor for the recombinant human IDO1-catalyzed dioxygenation reaction. Other hypohalous acids, generated in situ by lactoperoxidase (LPO) or in aqueous solutions of I_2 or Br_2, also activate IDO1. Contrastingly, the pseudohalide thoicyanate, a known, excellent substrate for LPO, yielded only trace levels of L-NFK. Importantly, complete conversion to L-NFK occurs with sub-stoichiometric hypohalous acid relative to L-Trp , and the overall reaction remains O_2-dependent. Kinetic analysis with variable L-Trp and multiple, fixed concentrations of the activators/ cofactors revealed typical Michaelis-Menten kinetics without substrate inhibition, which contrasts past analysis using alternative IDO1 assays. The calculated second order rate constants were overall comparable regardless of the identity and concentration of hypohalous acid. Finally, 1-methyl-L-tryptophan, a reported inhibitor and poor substrate for rhIDO1, was reexamined with the hypohalous acid-dependent conditions revealing an improved catalytic efficiency when compared with the native substrate L-Trp. Along with this unanticipated result, the in vivo functional and mechanistic implications of the newly discovered hypohalous acid-dependent IDO1 activity are discussed.

Significance

Indoleamine 2,3-dioxygenase-1 (IDO1) is a hemoprotein that catalyzes the conversion of L-tryptophan to *N′*-formyl-L-kynurenine (L-NFK). Past efforts have culminated in the conclusion that IDO1 is a checkpoint modulator of mammalian immunity, both in terms of the immunogenicity and immune tolerance. However, the identity of the endogenous activator of IDO1 is still unsettled. Here we report that sodium hypochlorite, aka bleach, activates ferric rhIDO1 in a catalytic manner, enabling rhIDO1 to efficiently catalyze the production of L-NFK in an O_2-dependent reaction. The results suggest rhIDO1 can efficiently operate via a hypochlorous acid-dependent mechanism that is reminiscent of the peroxide-shunt pathway used by other hemoproteins. Furthermore, the results suggest a functional role for endogenously produced hypochlorous acid beyond solely killing foreign pathogens.

INTRODUCTION

L-Tryptophan (L-Trp), an essential amino acid in the animal diet, is predominantly metabolized via the kynurenine (Kyn) pathway with estimations of 95% of consumed L-Trp being used in this capacity (*1*). Dysregulation or abnormalities of the Kyn pathway have been implicated in several pathologies including neurological diseases, psychiatric disorders, inflammatory conditions, and cancers, among many others (*2-4*). The first enzymatic step in the Kyn pathway, the oxidative conversion of L-Trp to *N'*-formyl-L-kynurenine (L-NFK), is catalyzed by one of three distantly related isozymes—tryptophan 2,3-dioxygenase (TDO), indoleamine 2,3-dioxygenase-1 (IDO1) or IDO2 (*5*) (Figure 1). Although still the subject of on-going research, the isozymes appear to have a distinct physiological distribution and function. IDO1 (EC 1.13.11.52), the focus of this study, is found in several tissues and is particularly over-produced in the placenta (*6-9*). The high placental abundance led to the initial discovery that IDO1 plays a pivotal role in immune tolerance, thereby protecting embryos from maternal immunity (*10,11*). Subsequent studies have revealed a role for IDO1 well beyond fetal development. Notably, IDO1 is produced at the highest levels in dendritic cells (DCs) (*12-16*) and to a lesser extent macrophages and eosinophils, where its expression is induced by lipopolysaccharide, interferon gamma, and other stimuli (*17-21*). The role of IDO1 in this immune cell population is generally believed to be twofold: *(i)* to starve invading microbes by depleting L-Trp and *(ii)* to produce metabolites initiating a signaling pathway that leads to immunosuppressive effects (*22*). The immunomodulatory properties are manifested in part through a suppression of the proliferation of cytotoxic and helper T cells and natural killer (NK) cells with concurrent upregulation of the production of regulatory T cells (Tregs) and myeloid-derived suppressor cells (*23-26*) (Figure 1). The extensive amount of data connecting IDO1 with a range of immunosuppressive outcomes, only briefly highlighted here, has led to the designation of IDO1 as a checkpoint modulator of immunity, both in terms of the immunogenicity and immune tolerance (*27-29*).

Initial studies with IDO1 isolated from the small intestine of *Oryctolagus cuniculus* (rabbit) led to the conclusion that the enzyme, initially called tryptophan pyrollase, is a

hemoprotein that functions as a dioxygenase, i.e. incorporates both O atoms of O_2 into the product L-NFK (*30-32*). Hemoproteins are a large family of mononuclear metalloproteins that contain an iron-bound porphyrin prosthetic group (i.e., heme) and can generally be categorized into two groups: those that directly engage with O_2 to fulfill their physiological function or those that utilize H_2O_2 (*33*). The former can be further broken down into the O_2-transport and storage proteins known as globins that includes myoglobin and hemoglobin and the O_2-dependent enzyme catalysts that function as either oxygenases or oxidases. The functional diversity of hemoproteins is dictated primarily by variations in the residues that make up the heme active site environment, perhaps none more important than the axial iron ligand that resides on the proximal side of the porphyrin ring. This residue, which is critical for fine-tuning the reduction potential of the metal center, is typically Cys for O_2-dependent enzymes that is exemplified by the well characterized family of cytochrome (CYP) P450 monooxygenases, which unlike IDO1, incorporate only one atom of O_2 into a substrate while reducing the other to H_2O (*34*). Studies with recombinant human protein (rhIDO1), first reported in 2000 (*35*), have identified a His as the proximal ligand (*36-38*). A proximal His is instead characteristic of the remaining types of hemoproteins: the H_2O_2-dependent peroxidases (with chloroperoxidase being a notable exception) and the O_2-binding globin family (*33,39*). Thus, IDO1 appears unique among hemoproteins by not only functioning catalytically as a dioxygenase but also by exploiting a His proximal ligand for engaging O_2 for catalysis.

Regardless of proximal ligand identity or the enzyme function, the commonly shared paradigm for O_2-binding hemoproteins involves iron in the ferrous (+2) oxidation state prior to engagement of O_2. For the globin family, the heme of the resting state—the default state before substrate binding— is predominantly the reduced, ferrous form. Contrastingly, the resting state of CYP P450 monooxygenases is predominantly in the oxidized, ferric heme. Consequently, CYP P450s require a separate reductase system to shuttle an electron into the heme to initiate substrate binding and the overall catalytic cycle. Evidence from in vivo and vitro studies suggest the resting state of human IDO1 is also the ferric heme (*35-38,40-42*). Based on the assumption that the established O_2-binding dogma is followed by IDO1, a single-electron reduction to ferrous iron would be

necessary for binding O_2 and initiating catalysis. This would occur despite the lack of need for any electron input for completing a catalytic cycle, i.e. the overall IDO1-catalyzed reaction is redox neutral. In early studies with rabbit IDO1, reduction was achieved in vitro by the addition of two components (termed cofactors at the time of discovery): the synthetic dye methylene blue (MB) and ascorbic acid (AA) (*31*,*43*). Alternatively, ferric heme reduction could be bypassed by chemically or enzymatically generating superoxide ($O_2^{\bullet-}$) (*43-45*). Reduced tetrahydrobiopterin (THBP) was also reported to substitute for MB/AA, thus providing a potential endogenous reductant for activating rabbit IDO1 for catalysis (*46*). Similarly to rabbit IDO1, human IDO1 uses the artificial MB/AA electron transport system to efficiently support catalysis (*47,48*). However, $O_2^{\bullet-}$ does not appear to support human IDO1 activity (*49*). Additionally, and in contrast to the activity for many CYP P450 monooxygenases, rhIDO1 was shown to be inoperable using a peroxide shunt pathway that employs H_2O_2 and ferric enzyme as a substitute for O_2 and the ferrous form of the enzyme (*50-52*). Indeed, assay conditions generally incorporate catalase to prevent H_2O_2-mediated inhibition. Polysulfides (*53*) and NADPH−cytochrome P450 reductase with or without cytochrome b_5 (*49,54,55*) have also been reported to support rhIDO1 catalytic activity in vitro. However, whether these reduction systems operate in vivo to support IDO1 catalysis is still unclear.

Of the many striking features of the IDO1-catalyzed reaction, we were intrigued by the conclusions that IDO1 and homologs are the only members of the proximal His hemoproteins that use O_2 as a substrate for a chemical transformation within the biological milieu. This was particularly interesting given the inability to definitively identify a palatable, endogenous “activator” (aka initiating factor) responsible for ferric heme reduction and hence O_2 engagement. We therefore set out to find operational parameters that, of critical importance, adequately reflect the physiological function of IDO1. Here we report the identification of a catalytically competent peroxidase-like shunt pathway for IDO1 that satisfies the activity-function connection. The key finding as reported herein is that sodium hypochlorite (NaOCl), aka bleach, activates ferric IDO1 in a catalytic manner. Further biochemical studies revealed that O_2 remains essential when using hypochlorite and that other hypohalites can support catalysis. The driving rationale and the

implications for the discovery of hypochlorite-mediated and O_2-dependent catalysis from the perspective of IDO1's physiological function in immunosuppression is discussed. Furthermore, a catalytic mechanism, which is not only consistent with the data presented here but is backed by strong literature precedent, is proposed that represents a new modus operandi for O_2 activation for hemoproteins.

RESULTS

Hypochlorite supports rhIDO1 catalysis. Activity of recombinant human IDO1 (rhIDO1) was initially examined in reactions using the artificial MB/AA electron transport system followed by heat workup to remove protein (Figure 2a). As expected, a new peak appeared in the HPLC-MS chromatogram that coincided with the disappearance of the L-Trp peak (Figure 2b). HRMS of the new peak, which had a distinct UV/VIS spectrum than reported for the known product of IDO1 (L-NFK), was consistent with the formation of (*E*)-4-[2-(formylamino)phenyl]-4-oxo-2-butenoic acid, the deamino derivative of L-NFK (dNFK) (Figure 2c). Sample work-up using ultrafiltration or trichloroacetic acid-mediated protein precipitation instead of boiling yielded a predominant peak eluting before L-Trp with UV/VIS and mass spectra consistent with L-NFK, demonstrating that dNFK is a degradation product due to heat treatment under mildly alkaline conditions. For reproducibility, all subsequent reactions were terminated by boiling, forming predominantly dNFK, but product yield was calculated based on both products (dNKF + unconverted L-NFK). By analyzing reactions following the complete conversion of several concentrations of L-Trp to dNFK + L-NFK [ε_{321nm} = 3750 $M^{-1}cm^{-1}$ (56)], the extinction coefficient of dNFK at 280 nm was determined to be 3075 $M^{-1}cm^{-1}$.

Neutrophils and macrophages undergo a respiratory burst in response to infection. This burst pathway involves three enzymes, NADPH oxidase, superoxide dismutase, and myeloperoxidase, that sequentially convert O_2 to $O_2^{\bullet-}$, H_2O_2, and HOCl, all of which are considered reactive oxygen species (ROS) capable of damaging invading microbes. Although often underappreciated, HOCl has also been demonstrated to have immunomodulatory properties via an unknown mechanism that alters cytokine signaling and suppresses inflammation in a manner that is uncannily like IDO1. With this insight and the knowledge that other heme-dependent enzymes (but, as previously noted, not rhIDO1) are known to use $O_2^{\bullet-}$ or H_2O_2 to bypass the need for ferric heme reduction, we tested the potential for ferric-heme rhIDO1 to use HOCl to catalyze the formation of L-NFK from L-Trp. HPLC analysis of rhIDO1 reactions using sodium hypochlorite (NaOCl;

100 μM) revealed reproducible conversion of L-Trp (1 mM) to dNFK. Freshly prepared hypochlorite solution from solid $Ca(OCl)_2$ was able to substitute for NaOCl. To confirm the reaction, lactoperoxidase (LPO; EC 1.11.1.7); an enzyme found in mammalian secretions such as milk, saliva, tears, and mucus which is commercially available from bovine milk; was employed for in situ generation of HOCl. Incubations of rhIDO1 and LPO with H_2O_2 and excess NaCl revealed formation of dNFK, although yields were substantially less in comparison to reactions starting directly with HOCl. Consistent with prior reports, rhIDO1 was inactive when substituting HOCl with H_2O_2 (Table S1) or using xanthine oxidase/xanthine to generate $O_2^{\bullet-}$ (and potentially $^{\bullet}OH$) in situ (57). In total, the data demonstrates that HOCl can support oxygenation for a heme-dependent enzyme analogous to the peroxide shunt reaction, although for rhIDO1 the reaction is highly specific for HOCl when compared to other endogenous ROS species.

Characterization of rhIDO1 activity with HOCl and potential substitutes. rhIDO1 reactions with 100 μM NaOCl and variable [AA] revealed a steady decline in enzyme activity when [AA] < 8 mM (Figure 3a), which was previously observed for IDO1 when using MB. At higher concentration of NaOCl (1 mM), substantially less AA was necessary for complete conversion to product (Figure 3a). Notably, at both concentrations of hypochlorite, reactions proceeded even in the absence of AA, suggesting AA enhances but is not essential for activity (Figure 3b). At constant AA (5 or 10 mM), an increase in activity was likewise observed upon increasing the concentrations of NaOCl or $Ca(OCl)_2$ with comparable conversion on a ^{-}OCl equivalency basis (Figure 3c and d). In contrast to reactions with variable [AA], however, no product was detected in the absence of HOCl. Furthermore, increasing the concentration of HOCl above 1 mM produced HPLC spectra with decreased substrate/product intensities and increased noise, probably due to the non-specific oxidative degradation of L-Trp and/or products. Using optimal concentrations, the highest product conversion was observed at pH of 7.4 (Figure S1). Notably, the equilibrium $^{-}OCl + H_2O \leftrightharpoons HOCl + {}^{-}OH$ (p*K*a = 7.5) exists roughly as a 1:1 mixture of ^{-}OCl and HOCl at pH = 7.4. For simplicity, all chlorine species are referred to as HOCl.

To probe halide selectivity, we next examined rhIDO1 activity using an LPO-coupled hypohalite/ hypothiocyanite generation system. LPO is known to catalyze the oxidation of Cl^-, Br^-, I^-, or the pseudohalide SCN^- in the presence of H_2O_2, thereby producing hypohalites or hypothiocyanite, respectively. All four (pseudo)halides successfully supported IDO1 catalysis, with the order of activity as follows: NaI ≈ KI > NaBr ≈ KBr >>> KCl ≈ KF ≈ KSCN (Figure 3e). This order is identical to the reported selectivity (based on second order rate constants) for bovine LPO alone except for one notable difference: KSCN is the preferred substrate for LPO (58). Thus, rhIDO1 appears selective toward true hypohalites. In contrast to reactions solely with rhIDO1, better conversion was observed in the absence of AA, suggesting AA potentially inhibits LPO, which has not been previously reported. Furthermore, the rhIDO1 reaction starting with NaOCl was inhibited by H_2O_2 as previously reported using MB/AA assay conditions. To avoid potential interference due to incompatibility with the LPO-coupled reaction conditions, rhIDO1 activity was tested with bromine water [Br_2 (*aq*)] and fresh preparations of I_2 (*s*) in water as a source of hypobromite and hypoiodite, respectively. Both solutions generate hypohalites that are formed via several pH-dependent reactions that are driven by kinetic and thermodynamic parameters. As expected, aqueous Br_2 and I_2 were effective substitutes for the LPO-coupled system with catalytic behavior identical to HOCl. However, the reaction rate and overall progress with 1 mM I_2 in solution was significantly greater than those observed with HOCl (Figure 3f). Assuming the equilibrium $I_2 + H_2O \leftrightharpoons HOI + I^- + H^+$ with $K_{eq} = 5.4 \times 10^{-13}$ M^2 dominates, reactions with1 mM I_2(aq) at pH 7.4 are equivalent to an initial concentration of $[HOI]_i$ = ~110 μM (the pK_a for HOI is estimated to be between 10.5-11). This amount of HOI in the presence of 5 mM AA and 1 mM L-Trp resulted in complete conversion of L-Trp to dNFK after 2.5 h (Figure 3f). Comparatively, conversion with 100 μM NaOCl was 12% (Figure 3c). With bromine water, assuming $Br_2 + H_2O \leftrightharpoons HOBr + Br^- + H^+$ with K_{eq} = ~5×10^{-9} M^2 so that $[HOBr]_i$ = ~992 μM (the pK_a for HOBr is 8.65), 2.5 h reactions with 5 mM AA gave 30% conversion which was increased to 100% with 10 mM AA (Figure 3g). Comparatively, conversion with 1 mM NaOCl was 100% at both AA concentrations. As noted above with NaOCl, reactions with concentrations > 1 mM of hypohalite source were difficult to interpret due to the loss of UV active species in the HPLC chromatograms. Finally, HOI and HOBr were generated

in situ by reacting NaOCl with NaI and NaBr, respectively. Nearly complete conversion was realized within 2.5 h when starting with 100 μM NaOCl and 1 mM L-Trp in the presence of 1 mM NaI (Figure 3h). Comparatively, conversion with 1 mM NaBr was 12% (Figure 3i), which is identical to reactions in the absence of NaBr (only NaOCl). Additionally, inclusion of NaI with NaOCl in reactions without AA approximately doubled the conversion of L-Trp to product (Figure 3b).

Taking into consideration the apparent distinct functional characteristics between IDO1 isolated from rabbit intestine versus the recombinant human form, the recombinant version from *Canis lupus dingo* was produced and purified from *E. coli*. A preliminary assessment revealed *Cd*IDO1, identically to rhIDO1, catalyzed the conversion of L-Trp to L-NFK using representative hypohalites (Figure S2). Thus, hypohalite-dependent IDO1 activity extends beyond humans and is potentially conserved across mammals.

Kinetic and TTN analysis. Single-substrate kinetic analysis with respect to variable [L-Trp] was next examined with the cofactors/activators that support rhIDO1 catalysis. The velocity plots followed Michaelis-Menten kinetics regardless of condition (Figure 4); the extracted kinetic parameters are summarized in Table 1. The second order rate constants are relatively close in value regardless of the identity or concentration of the cofactor/activator. An increase in K_m with respect to L-Trp is observed with increasing concentration of HOCl, which was off-set by a comparable fold-increase in k_{cat}. Consistent with our end-point assays suggesting no H_2O_2 inhibition, catalase—which catalyzes the conversion of H_2O_2 to H_2O and O_2 and is generally included in IDO1 assays by others—had no effect on the kinetic parameters when rhIDO1 was assayed with NaOCl. Finally, and likewise consistent with reported kinetic assays employing MB/AA, rhIDO1 catalyzes the reaction with D-Trp but has a significantly higher K_m when compared to the proteinogenic amino acid L-Trp.

Reassessment of 1-methyl-L-tryptophan, a reported IDO1 inhibitor and substrate. The substrate analogue 1-Me-DL-Trp has been described as a competitive inhibitor and alternative—albeit poor—substrate with respect to L-Trp when assayed with rhIDO1 and

the MB/AA conditions (59-61). Using the newly identified reaction conditions (200 μM NaOCl and heat workup), rhIDO1 reactions with commercially available 1-Me-L-Trp resulted in the loss of the peak corresponding to 1-Me-L-Trp and the appearance of a distinct peak with a λ_{max} at 227 nm and a shoulder at 278 nm with a broad tail extending to longer wavelengths (Figure S3). HRMS and NMR analyses of the purified product were consistent with the identity of the new peak as (*E*)-4-[2-(*N*-methylformamido)phenyl]-4-oxo-2-butenoic acid (*N*-Me-dNFK) (Figure S4). Inspection of the NMR spectrum suggested the product existing as a mixture of rotamers (2:1):(*E*:*Z*) at room temperature due to the restricted rotation about the N–C(O) bond. Increasing the temperature during acquisition of the ^{1}H-NMR spectrum resulted in the convergence of peaks at ~6.60 and ~7.35 ppm, providing evidence for this mixture of rotamers (Figure S4g). Furthermore, the *cis* relationship of the *N*-methyl group and the formyl hydrogen of the minor conformer was supported by NOESY (Figure S4f). Single-substrate kinetic analysis using HPLC to detect the product (Figure 4d and Table 1) revealed K_m = (8.6 ± 2.1) x 10^{-4} M^{-1} and k_{cat} = 37 ± 4 min^{-1}. This equates to a slight increase (1.3-fold) in the second order rate constant when compared to L-Trp under identical reaction conditions.

The detection of the putative rhIDO1 product prior to heat-induced deamination, *N′*-Me-L-NFK, was attempted using two prior methods routinely employed to quantitate rhIDO1 activity. Using the identical protocol with Ehlrich's reagent as described (59), the absorbance of the resulting chromophore at 480 nm was 9-times less than expected despite the completion of the reaction as judged by co-analysis using HPLC. Similarly, the extinction coefficient at 321 nm for *N′*-Me-L-NFK was calculated to be 408 $M^{-1}cm^{-1}$ (Figure S3), ~9-times less than the extinction coefficient for L-NFK ($\varepsilon_{321\ nm}$ = 3750 $M^{-1}cm^{-1}$) that we assume was previously used to calculate *N′*-Me-L-NFK concentration (61). In total, the data is consistent with past experiments underestimating the activity of IDO1 with *N′*-Me-L-NFK.

Preliminary mechanistic insight. As previously noted, complete conversion of 1 mM L-Trp to product was achieved with rhIDO1 (1-2 mM) and sub-stoichiometric (<1 mM) amounts of HOCl. By lowering the rhIDO1 concentration (0.05 mM), the total turnover

number (TTN) was estimated as ≥ 2000 when initiating the reaction with 100 μM or 500 μM of $Ca(OCl)_2$. Overall, this data suggests HOCl is not a substrate and is instead consistent with a role as an activator, i.e. gets consumed during the first catalytic cycle but is not required in subsequent cycles, or a cofactor, i.e. gets regenerated while participating in every catalytic cycle. This subsequently suggests that, as previously reported by others using MB/AA assay conditions, the source of both O atoms remains O_2 without incorporation of the O atom of the hypohalite. We attempted several times to demonstrate this using isotopic enrichment experiments following literature protocol and variations thereof but quickly realized that the solvent exchange with L-NFK was too rapid to provide meaningful data in our hands. Consequently, we simply examined whether O_2 was indeed required for reactions using the hypohalite conditions. For this purpose, solid I_2 was added to a thoroughly deoxygenated solution containing L-Trp, AA, and rhIDO1 and allowed to react under a nitrogen atmosphere for 4 hr. LCMS analysis revealed 7% of the starting material was converted to the product (Figure S5). In contrast, complete substrate conversion occurred in the control reaction, wherein the deoxygenated mixture (including IDO1) was opened to an O_2 atmosphere after I_2 addition (Figure S5). These results indicate that O_2 is still required for rhIDO1 catalysis in hypohalite conditions and likely remains the source of both O atoms in L-NFK, hence functioning as a dioxygenase.

Finally, rhIDO1 retained ≥80% of its activity following treatment with 1 mM potassium ferricyanide (III) (Figures 3b, c, and f – dashed lines). Therefore, HOCl-dependent rhIDO1 activity is unlikely to be initiated in the ferrous form despite still requiring O_2 to catalyze the conversion of L-Trp to L-NFK.

DISCUSSION

IDO1 catalyzes the O_2- and heme-dependent conversion of L-Trp to L-NFK to initiate the kynurenine pathway. Previous studies with IDO1 have independently revealed at least

three different electron reduction systems that are able to initiate IDO1 catalysis in vitro, namely MB/AA (48), hydrogen sulfide and polysulfides (53), or NADPH-cytochrome P450 reductase with or without cytochrome b_5 (49, 55). The function of each of these systems has been ascribed to regenerating and maintaining ferrous IDO1, which has been deemed the necessary form to achieve the dioxygenase activity. The data provided here demonstrate yet another way to achieve the rhIDO1-catalyzed conversion of L-Trp to L-NFK: catalytic initiation with hypohalous acids. This hypohalous acid-dependent activity is distinct from the other activation systems in that it altogether bypasses the need for generating the ferrous rhIDO1. Instead, this activation is reminiscent of peroxidases or the CYP P450 peroxide shunt pathway, although with key proposed mechanistic differences that are highlighted below. Nonetheless, to our knowledge, this is the first demonstration of a human enzyme that employs hypohalous acids for catalytic activation.

A major driving factor for examining rhIDO1 activity with hypohalous acids was consideration of the biological milieu that rhIDO1 is expected to function. A particularly formative driver was the work by Odobasic *et al*. that revealed MPO and more specifically, its product hypochlorous acid (and, importantly, not hydrogen peroxide) attenuates T cell driven tissue inflammation by “suppressing” the function of dendritic cells in draining lymph nodes (62). One of the many important findings of this work included that human monocyte-derived dendric cells cultured with neutrophil supernatants or MPO led to a significant decrease in HLA-DR and CD86 expression, both markers for productive T cell priming. Although many gaps remain to be addressed, the study provided compelling support for HOCl-driven immunomodulation via dendritic cell function. Likewise, studies have shown topical HOCl reduces inflammation and the pro-inflammatory response for many skin conditions including eczema, suggesting a role for rhIDO1 in this milieu as well (63). By activating rhIDO1, our data further supports that endogenous HOCl is more than a microbicidal agent, which is the predominant functional significance put forth in the community. In addition to these observations of HOCl immunomodulation, another driving factor for testing HOCl was the consideration of the three “flavors” of endogenous reactive oxygen species that are enzymatically formed during an immune response: $O_2^{\bullet-}$, H_2O_2, and HOCl (64). Interestingly, HOCl is often omitted and replaced with $^{\bullet}OH$ as one of these

three primary ROS (64,65). Both $O_2^{\bullet-}$ and H_2O_2 (via the peroxide shunt for CYP P450s or naturally with peroxidases) are known to substitute for O_2 and bypass the requisite 1-e^- reduction for initiating catalysis for many heme-containing enzymes (66). Although previously tested for binding and partial reactivity with myoglobin, horseradish peroxidase, and bovine catalase (67) and demonstrated as a reactive substrate with synthetic porphoryin mimics (68), HOCl is rarely (if ever) discussed as a potential oxidant for initiating heme-dependent chemistry. However, here we have shown that HOCl is the only ROS "flavor" used by rhIDO1 to generate L-NFK. Thus, it is tempting to speculate, at least in the scenario for dendritic cell function in draining lymph nodes, that HOCl functions as a signaling molecule by first entering dendritic cells, the established predominant factory for rhIDO1 production, and then activating rhIDO1 for concomitant depletion of L-Trp and formation of L-NFK. The presence or absence of these metabolites in turn ultimately regulate the differentiation of naïve T cells, a well-established connection to rhIDO1 activity.

The discovery that rhIDO1 uses HOCl to initiate multiple catalytic cycles re-opens the door for a new round of mechanistic studies on this intriguing enzyme family and potentially other hemoproteins. While we initially considered the possibility that the two O atoms of L-NFK originate from two HOCl equivalents for each catalytic cycle, the data are consistent with sub-stoichiometric HOCl with respect to L-Trp, suggesting HOCl is either a cofactor (i.e., re-formed at the end of each catalytic cycle) or activator. Furthermore, the HOCl-initiated reaction still requires O_2. Unfortunately, in contrast to reports by others (32,69), rapid solvent exchange of L-NFK prevented isotopically tracking the O atoms with acceptable rigor in our hands. Consequently, at this stage, we propose that HOCl initiates the catalytic cycle by ligation to the ferric heme in the distal pocket, which leads to a two-electron transfer to form Cl^- and a ferryl-oxo porphyrin radical cation, Compound I. From Compound I, minimally two pathways can be envisioned. The first exploits the oxidizing power of Compound I for abstraction of a π-electron from substrate L-Trp leading to a carbon-centered radical cation that directly reacts with triplet O_2. The subsequent peroxyl L-Trp radical is reduced followed by dioxetane formation leading to the rearrangement to form L-NFK. Reactions between carbon-centered radicals and O_2 to form hydroperoxides

are known to occur at rates near diffusion (k = 10^9-10^{10} $M^{-1}s^{-1}$) in solution (70). The reaction of O_2 during H_2O_2-mediated catalysis using metmyoglobin and methemoglobin from several sources lends support for this chemistry, as EPR studies suggest the formation of peroxyl radical at C3 of a L-Trp residue, which is likewise consistent with the formation of a C3 radical of the indole for rhIDO1 following HOCl-dependent Compound I genesis (71-74). Not surprisingly, the major peroxidation product of this L-Trp residue has been shown to be L-NFK (75). The intermediacy of a hydroperoxy species is further supported by analogous results examining chemical-sensitized photooxygenation (via the more relevant type I free radial mechanism or, alternatively, a type II singlet O_2 mechanism) of indole derivatives (76-78) including L-Trp residues in non-heme proteins (70, 79).

A provocative, alternative pathway for O_2 engagement is the direct reaction of the ferryl-oxo of Compound I with O_2 to transiently generate ozone (O_3) (Figure 5, path b). In this mechanism the O atom of the ferryl oxo could potentially be first reduced to the oxide radical ($\bullet O^-$) that then reacts with triplet O_2 to form a heme-ligated transient ozonide radical anion ($\bullet O_3^-$) and Compound II (not shown), the former of which is rapidly oxidized to O_3 with concomitant reduction of the latter to ferric rhIDO1. Importantly for the initiation of path b, experimental and computational analysis of horseradish peroxidase are consistent with a Compound I ground state having a triplet spin pair on the ferryl-oxo unit (80-83), suggesting that such a radical coupling is minimally spin-allowed. Subsequent ozonolysis of L-Trp to L-NFK would follow, a reaction which mimics the chemical synthesis employed for making L-NFK from L-Trp (84) and was determined chemically feasible in aqueous, neutral conditions by us (Figure S6). The IDO1-catalyzed reaction could potentially proceed through a molozonide and peroxide intermediates as shown, which is based on NMR analysis of the synthetic reactions. Peroxide reduction by Cl^- to form L-NFK would regenerate the HOCl-ligated ferric rhIDO1. Central to this mechanism is the ability of rhIDO1 to generate O_3, an entity that is typically considered in the context of atmospheric chemistry but not biological systems. Although the standard reduction potential of O_3 is indeed relatively high, it is still less than the hydroxyl radical, •OH (notably of which is the conjugate acid of the oxide radical that is proposed here) that has

been reported as a product of several hemoproteins when exposed to H_2O_2 under suboptimal or uncoupling conditions, including horseradish peroxidase (85) and others. The estimated difference in standard reduction potential in water between H_2O_2 and •OH (1.78 V and 2.80 V, respectively) is significantly greater than HOCl and O_3 (1.48 V, acid form and 2.08 V, respectively), suggesting the HOCl-O_3 couple is feasible when simply considering the comparable thermodynamic barriers (86). Finally, while ozonolysis has been demonstrated to convert L-Trp residues to the corresponding L-NFK residues and degrade heme prosthetic groups in vitro (87-89), the endogenous production of O_3, and the potential for an in vivo function, has not been widely accepted. Several noncatalytic processes using alternative ROS have been proposed to generate O_3 (90), but perhaps most intriguing is the proposal of catalytic antibody-mediated O_3 production (91-93) and that the HOCl-producing enzyme MPO plays an important role in this catalytic process (93). With respect to function, this ozone generation has been proposed to occur in neutrophils, consistent with a role in the immune response. In support of an immunosuppressive role for O_3, it is interesting to note that medical ozone therapy, although not FDA approved in the US, has been used throughout the world to manage many chronic inflammatory diseases including MS and arthritis.

Following the discovery of the HOCl-dependent IDO1 activity, we initiated studies to re-assess perceived substrates and inhibitors that were identified using the MB/AA assay system. Here we report the results from one of these, 1-Me-DL-Trp, which has been the source of confusing if not contradicting data during its development as therapeutic agent. When human rIDO1 was first characterized in vitro, 1-Me-DL-Trp was concluded to be a poor substrate relative to L-Trp (7% relative conversion to an unidentified product) and a relatively strong inhibitor (limited L-Trp conversion to 27%) when using Ehlrich's reagent to detect product formation (59). A later study using the same workup conditions revealed differences between the enantiomers, with 1-Me-L-Trp behaving as a competitive inhibitor with respect to L-Trp (K_i = 19 mM) unlike the D-isomer (K_i > 100 mM) (60). Unexpectedly, the L-isomer, in contrast to the D-isomer, was shown to have poor immunosuppression properties in vivo in the same study (60).

A more recent assessment of rhIDO1 led to the conclusion that 1-Me-L-Trp is indeed a substrate with the identity of the product being supported, for the first time, by low resolution LC-MS (87). Single-substrate kinetic analysis by monitoring product formation at 321 nm suggested that 1-Me-L-Trp was a relatively poor substrate with K_m = 150 +/- 11 μM and k_{cat} = 0.027 +/- 0.001 s^{-1}, approximately 9 x 10^{-4} the catalytic efficiency in comparison to the reaction with L-Trp (61) Using HPLC with diode array as a primary detection method along with a thorough spectroscopic analysis of the degradation product, we confirmed here that 1-Me-L-Trp is indeed a substrate using the newly discovered HOCl-dependent assay conditions. However, our data suggests 1-Me-L-Trp is actually as good as, if not better substrate than L-Trp. With this realization, the detection methods previously employed were reassessed, which revealed that *N'*-Me-L-NFK formation was likely greatly underestimated. Based on these results, it is thus tempting to speculate that prior failure to move 1-Me-L-Trp forward as an immunomodulatory therapeutic is a consequence of being efficiently converting 1-Me-L-Trp in vivo by rhIDO1, potentially to a product that behaves similarly in vivo to L-NFK. It will now be interesting to test whether this is indeed the case. Furthermore, we expect that the assay blueprint established here can now serve as the foundation for re-examining other categorized inhibitors and/or substrates, including D-isomer of 1-Me-Trp. Finally, from a mechanistic perspective, the turnover improvement with 1-Me-L-Trp is speculated to be attributed to the electron-donating group inductive effect, which supports the reactivity of hypothetical intermediates for both paths in Figure 5.

Neutrophils and macrophages generate HOCl in response to foreign insults. The long-standing and widespread rationale for this HOCl production is to serve the singular role of killing invading organisms. Not surprisingly, a substantial amount of time and effort has been dedicated to understanding the killing mechanism therein. Our data provides evidence for an additional role for HOCl by activating the enzyme rhIDO1, a key immune response modulator. Consequently, the results suggest a new signaling pathway in immunomodulation, paving the way for downstream studies to explore the biological implications of this newfound HOCl-IDO1 immunomodulation connection. Just as significant are the mechanistic implications for catalysis. To our knowledge this is the first

example of an enzyme that can use HOCl to complete an oxygenation cycle. We hypothesize HOCl is used to generate a Compound I intermediate (both paths) and potentially Compound II (path b), the latter of which has been reportedly observed with Raman spectroscopy and IDO1 prepped in distinct conditions to that reported here (41,42,94). Interestingly, this HOCl-mediated IDO1 catalysis is in contrast to results exploring a potential peroxide shunt using H_2O_2, which has led to the conclusion that H_2O_2 facilitates the formation of a ferryl species resembling Compound I (50,51) or Compound II (95) yet does not impart IDO1 the ability to transform L-Trp to L-NFK. Furthermore, it is intriguing to speculate that the hypohalite-shunt might not be limited to rhIDO1, with other proximal His- or perhaps proximal Cys-hemoproteins potentially being able to operate in a similar manner (67). Interestingly, LPO in the resting state is already known to convert HOCl to Compound I, in what is essentially the reverse reaction (58). Finally, we are proposing that the ferrous heme is not required, hence exploits the shunt-like pathway in such a manner that O_2 is not a direct, heme ligand during the catalytic cycle. This last proposal runs counter to the apparently universally accepted paradigm for heme-dependent oxygenases. However, nature has demonstrated multiple other heme-independent strategies to activate O_2, including oxygenases such as iron-independent flavin-dependent enzymes exemplified by glucose oxidase, ferric-hydroxide-dependent lipoxygenases, and so-called cofactorless oxygenases, among others. It will now be of mechanistic interest to probe the O_2 activation hypothesis and reconcile this new IDO1 activity with the wealth of data already available in the public domain on this fascinating enzyme.

METHODS

Materials were from standard sources and used without further purification. The recombinant human IDO1 (rhIDO1) was produced and purified using standard conditions. Routine assays (identified as optimal conditions) were carried out in a 100 mM potassium phosphate buffer (pH = 7.4), 5-10 mM ascorbic acid (AA), 1 mM L-Trp, 0.2-1 mM HOCl, and 0.4 μM rhIDO1. Reactions were performed in an open atmosphere at room temperature. Kinetic data were fitted to the Michaelis-Menten equation using GraphPad Prism 10 to extract parameters. Detailed protein purification protocol, assay conditions including for kinetic analysis, HPLC methods, and production and characterization of *N*-Me-dNFK are provided in the online supporting information.

ACKNOWLEDGEMENTS

Parts of this work were supported by NIH P20GM130456 COBRE for Translational Chemical Biology.

REFERENCES

1. C. Xue *et al*., Tryptophan metabolism in health and disease. *Cell Metab.* ***35***, 1304-1326 (2023).
2. M. Platten, E. A. A. Nollen, U. F. Röhrig, F. Fallarino, C. A. Opitz, Tryptophan metabolism as a common therapeutic target in cancer, neurodegeneration and beyond. *Nat. Rev. Drug Discov.* **18**, 379-401 (2019).
3. M. Dehhaghi, H. Kazemi, S. Panahi, G. J. Guillemi, Microorganisms, tryptophan metabolism, and kynurenine pathway: A complex interconnected loop influencing human health status. *Int. J. Tryptophan Res.* **12**, 1-10 (2019).
4. F. Moroni, Tryptophan metabolism and brain function: focus on kynurenine and other indole metabolites. *Eur. J. Pharmacol.* **375**, 87-100 (1999).
5. Q. Zhou, Y. Shi, C. Chen, F. Wu, Z. Chen, A narrative review of the roles of indoleamine 2,3-dioxygenase and tryptophan-2,3-dioxygenase in liver diseases. *Ann. Transl. Med.* **9**, 174 (2021).
6. I. Théate *et al.*, Extensive profiling of the expression of the indoleaomine 2,3-dioxygenases 1 protein in normal and tumoral human tissues. *Cancer Immunol. Res.* **3**, 161-172 (2015).
7. X. Dai, B. T. Zhu, Indoleamine 2,3-dioxygenase tissue distribution and cellular localization in mice: implications for its biological functions. *J. Histochem. Cytochem.* **58**, 17-28 (2010).
8. Y. Kudo, Indoleamine 2,3-dioxygenase: distribution and function in the developing human placenta. *J. Reprod. Immunol.* **61**, 87-98 (2004).
9. F. Yamazaki, T. Kuroiwa, O. Takikawa, R. Kido, Human indolylamine 2,3-dioxygenase. Its tissue distribution, and characterization of the placental enzyme. *Biochem. J.* **230**, 635-638 (1985).
10. D. H. Munn *et al.*, Prevention of allogeneic fetal rejection by tryptophan catabolism. *Science*. **281**, 1191-1193 (1998).
11. A. Hönig *et al.*, Indoleamine 2,3-dioxygenase (IDO) expression in invasive extravillous trophoblast supports role of the enzyme for materno-fetal tolerance. *J Reprod Immunol*. **61**, 79-86 (2004).
12. F. Fallarino, *et al.*, Functional expression of indoleamine 2,3-dioxygenase by murine CD8α^+ dendritic cells. *Internat. Immunol.* **14**, 65-68 (2002).
13. A. L. Mellor *et al.*, Induced indoleamine 2,3 dioxygenase expression in dendritic cell subsets suppresses T cell clonal expansion. *J. Immunol*. **171**, 1652-1655 (2003).
14. A. L. Mellor, D. B. Keskin, T. Johnson, P. Chandler, D. H. Munn, Cells expressing indoleamine 2,3-dioxygenase inhibit T cell responses. *J. Immunol.* **168**, 3771-3776 (2002).
15. S. L. Hwang, N. P.-Y. Chung, J. K.-Y. Chan, C.-L. S. Lin, Indoleamine 2,3-dioxygenase (IDO) is essential for dendritic cell activation and chemotactic responsiveness to chemokines. *Cell Res.* **15**, 167-175 (2005).
16. D. H. Munn *et al.*, Expression of indoleamine 2,3-dioxygenase by plasmacytoid dendritic cells in tumor-draining lymph nodes. *J. Clin. Invest.* **114**, 280-290 (2004).
17. S. O. Odemuyiwa *et al.*, Human eosinophils regulate T cell subset selection through indoleamine 2,3-dioxygenase. *J. Immunol.* **173**, 5909-5913 (2004).

18. S. Astigiano *et al.*, Eosinophil granulocytes account for indoleamine 2,3-dioxygenase-mediated immune excape in human non-small cell lung cancer. *Neoplasia*, **7**, 390-396 (2005).
19. R. Yoshida, O. Hayaishi, Induction of pulmonary indoleamine 2,3-dioxygenase by intraperitoneal injection of bacterial lipopolysaccharide. *Proc. Natl. Acad. Sci. USA.* **75**, 3998-4000 (1978).
20. R. Yoshida, J. Imanishi, T. Oku, T. Kishida, O. Hayaishi, Induction of pulmonary indoleamine 2,3-dioxygenase by interferon. *Proc. Natl. Acad. Sci. USA.* **78**, 129-132 (1981).
21. O. Takikawa, Y. Tagawa, Y. Iwakura, R. Yoshida, R. J. Truscott, Interferon-gamma-dependent/independent expression of indoleamine 2,3-dioxygenase: Studies with interferon-gamma-knockout mice. *Adv. Exp. Med. Biol.* **467**, 553-557 (1999).
22. A. Müller *et al.*, The missing link between indoleamine 2,3-dioxygenase mediated antibacterial and immunoregulatory effects. *J. Cell. Mol. Med*. **13**, 1125-1135 (2008).
23. B. Baban *et al.*, IDO activates regulatory T cells and blocks their conversion into T_H17-like T cells. *J. Immunol.* **183**, 2475-2483 (2009).
24. M. J. Forteza *et al.*, Activation of the regulatory T-cell/indoleamine 2,3-dioxygenase axis reduces vascular inflammation and atherosclerosis in hyperlipidemic mice. *Front. Immunol.* **9**, 950 (2018).
25. L. M. F Merlo *et al.*, Differential roles of IDO1 and IDO2 in T and B cell inflammatory immune responses. *Front. Immunol.* **11**, 1861 (2020).
26. S. M. Lightman *et al.*, Indoleamine 2,3-dioxygenase 1 is essential for sustaining durable antibody responses. *Immunity* **54**, 2772-2783 (2021).
27. H. de la Fuente *et al.*, Immunoregulatory molecules are master regulators of inflammation during the immune response. *FEBS Lett.* **586**, 2897-2905 (2012).
28. I. Mellman, Dedritic cells: Master regulators of the immune response. *Cancer Immunol. Res.* **1**, 145-149 (2013).
29. G. C. Prendergast, Immune escape as a fundamental trait of cancer: focus on IDO1. *Oncogene* **27**, 3889-3900 (2008).
30. S. Yamamoto, O. Hayaishi, O. Tryptophan pyrrolase of rabbit intestine. D- and L-tryptophan-cleaving enzyme or enzymes. *J. Biol. Chem.* **242**, 5260-5266 (1967).
31. Shimizu, T.; Nomiyama, S.; Hirata, F.; Hayaishi, O.; Indoleamine 2,3-dioxygenase. Purification and some properties. *J. Biol. Chem.* **1978**, *253*, 4700-4706.
32. O. Hayaishi *et al.*, Indoleamine 2,3-dioxygenase. Incorporation of $^{18}O_2^-$ and $^{18}O_2$ into the reaction products. *J. Biol. Chem.* **252**, 3548-3550 (1977).
33. T. L. Poulos, Heme enzyme structure and function. *Chem. Rev.* **114**, 3919-3962 (2014).
34. F. P. Guengerich, Mechanisms of cytochrome P450-catalyzed oxidations. *ACS Catalysis* **8**, 10964-10976 (2018).
35. T. K. Littlejohn *et al.*, Expression and purification of recombinant human indoleamine 2,3-dioxygenase. *Protein Expr. Purif.* **19**, 22-29 (2000).
36. T. K. Littlejohn, O. Takikawa, R. J. W. Truscott, M. J. Walker, Asp^{274} and His^{346} are essential for heme binding and catalytic function of human indoleamine 2,3-dioxygenase. *J. Biol. Chem.* **278**, 29525-29531 (2003).

37. H. Sugimoto *et al.*, Crystal structure of human indoleamine 2,3-dioxygenase: Catalytic mechanism of O_2 incorporation by a heme-containing dioxygenase. *Proc. Natl. Acad. Sci. USA.* **103**, 2611-2616 (2006).
38. N. D. Papadopoulou *et al.*, Redox and spectroscopic properties of human indoleamine 2,3-dioxygenase and a His303Ala variant: Implications for catalysis. *Biochemistry* **44**, 14318-14328 (2005).
39. I. I. Vlasova, Peroxidase activity of human hemoproteins: Keeping the fire under control. *Molecules* **23**, 2561 (2008).
40. M. Nakagawa *et al.*, A valid model for the mechanism of oxidation of tryptophan to formylkynurenine—25 years later. *Proc. Natl. Acad. Sci. USA.* **74**, 4730-4733 (1977).
41. A. Lewis-Ballester *et al.*, Evidence for a ferryl intermediate in a heme-base dioxygenase. *Proc. Natl. Acad. Sci. USA.* **106**, 17371-17376 (2009).
42. S. Yanagisawa *et al.*, Identification of the Fe-O_2 and the Fe=O species for indoleamine 2,3-dioxygenase during catalytic turnover. *Chem. Lett.* **39**, 36-37 (2010).
43. M. Sono, The roles of superoxide anion and methylene blue in the reductive activation of indoleamine 2,3-dioxygenase by ascorbic acid or by xanthine oxidase-hypoxanthine. *J. Biol. Chem.* **264**, 1616-1622 (1989).
44. T. Taniguchi, M. Sono, F. Hirata, O. Hayaishi, Indoleamine 2,3-dioxygenase. Kinetic studies on the binding of superoxide anion and molecular oxygen to enzyme. *J. Biol. Chem.* **254**, 3288-3294 (1979).
45. F. Hirata, O. Hayaishi, Studies on indoleamine 2,3-dioxgyenase. I. Superoxide anion as a substrate. *J. Biol. Chem.* **250**, 5960-5966 (1975).
46. M. Nishikimi, A function of tetrahydropteridines as cofactors for indoleamine 2,3-dioxygenase. *Biochem. Biophys. Res. Comm.* **63**, 92-98 (1975).
47. F. Yamazaki, T. Kuroiwa, O. Takikawa, R. Kido, R. Human indolylamine 2,3-dioxygenase. Its tissue distribution, and characterization of the placental enzyme. *Biochem. J.* **230**, 635-638 (1985).
48. C. J. D. Austin *et al.*, Optimized expression and purification of recombinant human indoleamine 2,3-dioxygenase. *Protein Expr. Purif.* **37**, 392-398 (2004).
49. G. J. Maghzal, R. R. Thomas, N. H. Hunt, R. Stocker, Cytochrome b_5, not superoxide anion radical, is a major reductant of indoleamine 2,3-dioxygnease in human cells. *J. Biol. Chem.* **283**, 12014-12025 (2008).
50. M. Freewan *et al*., Human indoleamine 2,3-dioxygenase is a catalyst of physiological heme peroxidase reactions. Implications for the inhibition of dioxygenase activity by hydrogen peroxide. *J. Biol. Chem.* **288**, 1548-1567 (2013).
51. H. H. Kuo, A. G. Mauk, Indole peroxygenase activity of indoleamine 2,3-dioxygenase. *Proc. Natl. Acad. Sci. USA.* **109**, 13966-13971 (2012).
52. C. Lu, S.-R. Yeh, Ferryl derivatives of human indoleamine 2,3-dioxygenase. *J. Biol. Chem.* **286**, 21220-21230 (2011).
53. M. T . Nelp, V. Zheng, K. M. Davis, W. K. J. Stiefel, J. T. Groves, Potent activation of indoleamine 2,3-dioxygenase by polysulfides. *J. Am. Chem. Soc.* **141**, 15288-15300 (2019).
54. E. Vottero *et al.*, Cytochrome b_5 is a major reductant in vivo of human indoleamine 2,3-dioxygenase expressed in yeast. *FEBS Lett.* **580**, 2265-2268 (2006).
55. J. T. Pearson, S. Siu, D. P. Meininger, L. C. Wienkers, D. A. Rock, In vitro modulation of cytochrome P450 reductase supported indoleamine 2,3-dioxygenase activity by

allosteric effectors cytochrome b_5 and methylene blue. *Biochemistry* **49**, 2647-2656 (2010).
56. A. H. Mehler, W. E. Knox, The conversion of tryptohan to kynurenine in liver II. The enzymatic hydrolysis of formylkynurenine. *J. Biol. Chem.* **187**, 431-438 (1950).
57. P. Kuppusamy, J. L. Zweier, Characterization of free radical generation by xanthine oxidase. Evidence for hydroxyl radical generation. *J. Biol. Chem.* **264**, 9880-9884 (1989).
58. P. G. Furtmüller *et al*., Reaction of lactoperoxidase compound I with halides and thiocyanate. *Biochemistry* **41**, 11895-11900 (2002).
59. M. D. Southan *et al.*, Structural requirements of the competitive binding site of recombinant human indoleamine 2,3-dioxygenase. *Med. Chem. Res.* **6**, 343-352 (1996).
60. D.-Y. Hou et al., Inhibition of indoleamine 2,3-dioxygenase in dendritic cells by stereoisomers of 1-methyl-tryptophan correlates with antitumor responses. *Cancer Res.* **67**, 792-801 (2007).
61. M. Chauhan et al., Reassessment of the reaction mechanism in the heme dioxygenases. *J. Am. Chem. Soc.* **131**, 4186-4187 (2009).
62. D. Odobasic *et al*., Neutrophil myeloperoxidase regulates T-cell-driven tissue inflammation in mice by inhibiting dendritic cell function. *Blood*, **121**, 4195-4204 (2013).
63. T. H. Leung *et al*., Topical hypochlorite ameliorates NF-κB–mediated skin diseases in mice. *J. Clin. Invest.* **123**, 5361–5370 (2013).
64. X. Li, Precise modulation and use of reactive oxygen species for immunotherapy. *Sci. Adv*. **10**, eadl0479 (2024).
65. A. J. Pontes Oliveira de Almeida et al., ROS: Basic concepts, sources, cellular signaling, and its implications in aging pathways. *Oxid. Med. Cell. Longev.* **2022** Article ID 1225578 (2022).
66. A. W. Munro, H. M. Girvan, A. E. Mason, A. J. Dunford, K. J. McLean, What makes a P450 tick? *Trends Biochem. Sci.* **38**, 140-150 (2013).
67. S. Ozaki, C. Dairaku, Y. Kuradomi, J. Inoue, The reaction of hemoproteins with hypochlorous acid. *Chem. Lett.* **37**, 666-667 (2008).
68. Z. Cong, S. Yanagisawa, T. Kurahashi, T. Ogura, S. Nakashima, H. Fujii, Synthesis, characterization, and reactivity of hypochloritoiron(III) porphyrin complexes. *J. Am. Chem. Soc.* **134**, 20617-20620 (2012).
69. J. Basran *et al.*, The mechanism of formation of N-formylkynurenine by heme dioxygenases. *J. Am. Chem. Soc.* **133**, 16251-16257 (2011).
70. M. J. Davies, Protein oxidation and peroxidation. *Biochem. J.* **473**, 805-825 (2016).
71. M. R. Gunther, D. J. Kelman, J. T. Corbett, R. P. Mason, Self-peroxidation of metmyoglobin results in formation of an oxygen-reactive tryptophan-centered radical. *J. Biol. Chem.* **270**, 16075–16081 (1995).
72. J. A. DeGray, Peroxidation of a specific tryptophan of metmyoglobin by hydrogen peroxide. *J. Biol. Chem.* **272**, 2359–2362 (1997).
73. M. J. Davies, Detection of myoglobin-derived radicals on reaction of metmyoglobin with hydrogen peroxide and other peroxidic compounds. *Free Rad. Res. Commun.* **10**, 361-370 (1990).

74. B. J. Reeder, D. A. Svistunenko, C. E. Cooper, M. T. Wilson, The radical and redox chemistry of myoglobin and hemoglobin: from in vitro studies to human pathology. *Antioxid. Redox Signal.* **6**, 954-966 (2004).
75. B. J. Reeder, D. A. Svistunenko, M. A. Sharpe, M. T. Wilson, Characteristics and mechanism of formation of peroxide-induced heme to protein cross-linking in myoglobin.
Biochemistry **43**, 10475–10486 (2004).
76. I. Saito, T. Matsuura, M. Nakagawa, T. Hino, Peroxidic intermediates photosensitized oxygenation of tryptophan derivatives. *Acc. Chem. Res.* **10**, 346-352 (1977).
77. E. Silva *et al.*, Riboflavin-induced type 1 photoxidation of tryptophan using a high intensity 365 nm light emitting diode. *Free Rad. Biol. Med.* **131**,131-143 (2019).
78. G. E. Ronsein, M. C. B. D. Oliveria, S. Miayjoto, M. H. G. D. Medeiros, P. D. Mascio, Tryptophan oxidation by singlet moldeulcar oxygen [O_2 ($^1\Delta_g$)]: Mechanistic Studies using ^{18}O-labeled hydroperoxides, mass spectrometry, and light emission measurements. *Chem. Res. Toxicol.* **21**, 1271-1283 (2008).
79. J. A. Silvester, G. S. Timmins, M. J. Davies, Protein hydroperoxides and carbonyl groups generated by porphyrin-induced photo-oxidation of bovine serum albumin. *Arch. Biochem. Biophys.* **350**, 249-258 (1998).
80. J. E. Roberts, B. M. Hoffman, R. Rutter, L. P. Hager, Electron-nuclear double resonance of horseradish peroxidase compound I. Detection of the porphyrin pi-cation radical. *J. Biol. Chem*. **256**, 2118-2121 (1981).
81. J. E. Roberts, B. M. Hoffman, R. Rutter, L. P. Hager, Oxygen-17 ENDOR of horseradish peroxidase compound I. *J. Am. Chem. Soc.* **103**, 7654-7656 (1981).
82. E. Derat, S. Cohen, S. Shaik, A. Altun, W. Thiel, Principal active species of horseradish peroxidase, Compound I: A hybrid quantum mechanical/molecular mechanical study. *J. Am. Chem. Soc.* **127**, 13611-13621 (2005).
83. C. E. Schulz, R. Rutter, J. T. Sage, P. G. Debrunner, L. P. Hager, Mössbauer and electron paramagnetic resonance studies of horseradish peroxidase and its catalytic intermediates. *Biochemistry*, **23**, 4743–4754 (1984).
84. F. Sakiyama, N. Masuda, T. Nakazawa, Y. Katsuragi, Quantitative ozone-oxidation of tryptophan to *N'*-formylkynurenine and kynurenine. *Chem. Lett.* **7**, 893-896 (1978).
85. T. Miura, A mechanistic study of the formation of hydroxyl radicals induced by horseradish peroxidase with NADH. *J. Biochem.* **152**, 199-206 (2012).
86. J. Kucera, Biofouling of polyamide membranes: Fouling mechanisms, current mitigation and cleaning strategies, and future prospects. *Membranes* **9**, 111 (2019).
87. J. B. Mudd, R. Leavitt, A. Ongun, T. T. McManus, Reaction of ozone with amino acids and proteins. *Atmos. Environ.* **3**, 669-682 (1969).
88. A. Previero M. A. Coletti-Previero MA, P. Jollès, Localization of non-essential tryptophan residues for the biological activity of lysozyme. *J. Mol. Biol.* **24**, 261-268 (1967).
89. F. Cataldo, Ozone degradation of biological molecules: Proteins, hemoglobin, RNA, and DNA. *Ozone. Sci. Eng.* **28**, 317-328 (2006).
90. A. N. Onyango, Endogenous ozone as a regular reactive oxygen species in (patho) physiology. *Adv. Redox Res.* **9**, 100075 (2023).

91. B. M. Babior, C. Takeuchi, J. Ruedi, A. Gutierrez, P. J. Wentworth, Investigating antibody-catalyzed ozone generation by human neutrophils. *Proc Natl Acad Sci USA.* **100**, 3031-3034 (2003).
92. J. Nieva, P. J. Wentworth, The antibody-catalyzed water oxidation pathway–a new chemical arm to immune defense? *Trends Biochem. Sci.* **29**, 274-278 (2004).
93. S. Tomono *et al.*, Formation of cholesterol ozonolysis products in vitro and in vivo through a myeloperoxide-dependent pathway. *J. Lipid Res.* **52**, 87-97 (2011).
94. E. S. Booth, J. Basran, M. Lee, S. Handa, E. L. Raven, Substrate oxidation by indoleamine 2,3-dioxygenase. *J. Biol. Chem.* **290**, 30924-30930 (2015).
95. C. Lu, S.-R. Yeh, Ferryl derivatives of human indoleamine 2,3-dioxygeanse. *J. Biol. Chem.* **286**, 21220-21230 (2011).

TABLES

Table 1. Single substrate kinetic parameters for rhIDO1.

Substrate	Activator/Cofactor (concentration)	K_m (M)	k_{cat} (min^{-1})	k_{cat}/K_m (relative)
L-Trp	NaOCl (200 μM)	$(1.8 \pm 0.5) \times 10^{-4}$	6.0 ± 0.4	1
	NaOCl (200 μM) + catalase[a]	$(2.0 \pm 0.6) \times 10^{-4}$	6.2 ± 0.4	0.94
	$Ca(OCl)_2$ (100 μM)	$(5.5 \pm 1.2) \times 10^{-4}$	10.4 ± 0.7	0.56
	NaOCl (1 mM)	$(1.1 \pm 0.4) \times 10^{-3}$	29 ± 4	0.79
	$Ca(OCl)_2$ (500 μM)	$(1.2 \pm 0.4) \times 10^{-3}$	29 ± 4	0.73
	I_2 (1 mM)	$(1.5 \pm 0.6) \times 10^{-3}$	21 ± 4	0.42
	Br_2 (1 mM)	$(4.7 \pm 0.9) \times 10^{-4}$	19 ± 1	1.2
	$Ca(OCl)_2$ (100 μM) + NaBr[b]	$(5.2 \pm 1.8) \times 10^{-4}$	8.0 ± 0.7	0.46
D-Trp	$Ca(OCl)_2$ (100 μM)	$\geq(5.9 \pm 1.6) \times 10^{-3}$	≥180 ± 35	0.9
1-Me-L-Trp	NaOCl (200 μM)	$(8.6 \pm 2.1) \times 10^{-4}$	37 ± 4	1.3

[a]10 μg/mL; [b]100 μM.

FIGURES

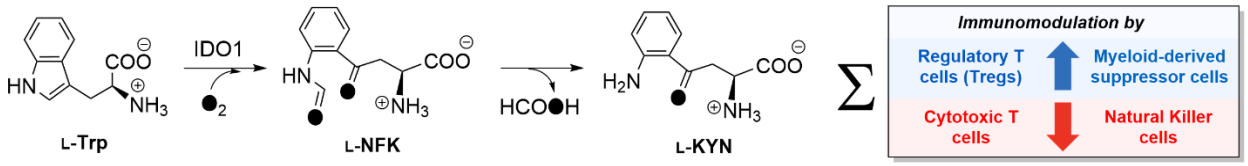

Figure 1. Reaction catalyzed by indoleamine 2,3-dioxygenase-1 (IDO1) and representative immunomodulatory outcomes linked to the IDO1. IDO1 catalyzes the L-tryptophan (L-Trp)- and O_2-dependent formation of *N′*-formyl-L-kynurenine (L-NFK), which is hydrolyzed noncatalytically or by a distinct enzyme (arylformamidase, E.C. 3.5.1.9) to generate formic acid and L-kynurenine (L-KYN).

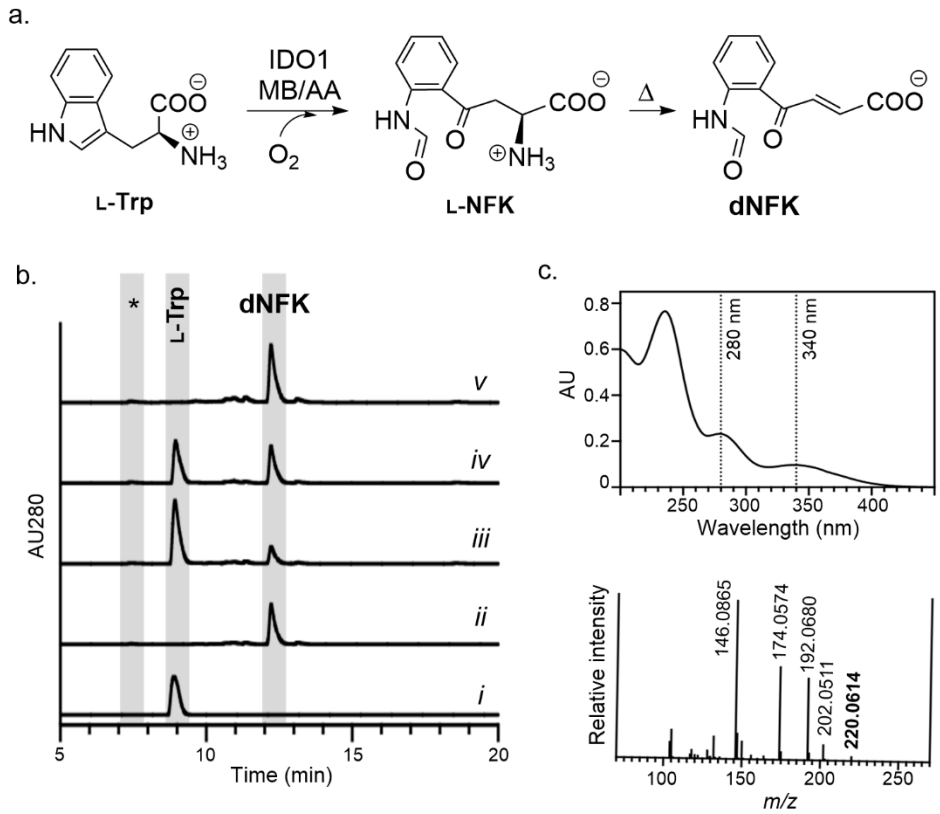

Figure 2. Reaction catalyzed by indoleamine 2,3-dioxygenase-1 (IDO1). (a) The established IDO1 reaction using methylene blue (MB) and ascorbic acid (AA) to form *N′*-formyl-L-kynurenine (L-NFK), which can degrade to the deamino derivative dNFK. (b) HPLC traces of the rhIDO1-catalyzed reaction including the control (no enzyme, trace *i*); rhIDO1 reaction for 2.5 h using established conditions with MB/AA (trace *ii*); rhIDO1 reaction for 2.5 h with 1 mM L-Trp, 100 μM NaOCl, and 10 mM AA (trace *iii*); rhIDO1 reaction for 2.5 h with 1 mM L-Trp, 100 μM $Ca(OCl)_2$, and 10 mM AA (trace *iv*); and rhIDO1 reaction for 14 h with 1 mM L-Trp, 100 μM $Ca(OCl)_2$, and 10 mM AA (trace *v*);. AU280, absorbance units at 280 nm; *, retention time for L-NFK, which has minimal absorbance at 280 nm. (c) Spectroscopic analysis of dNFK including the UV/VIS spectrum and high-resolution mass spectrum in positive mode (calculated *m/z* = 220.0610 for $[C_{11}H_9NO_4 + H]^+$ ion corresponding to dNFK).

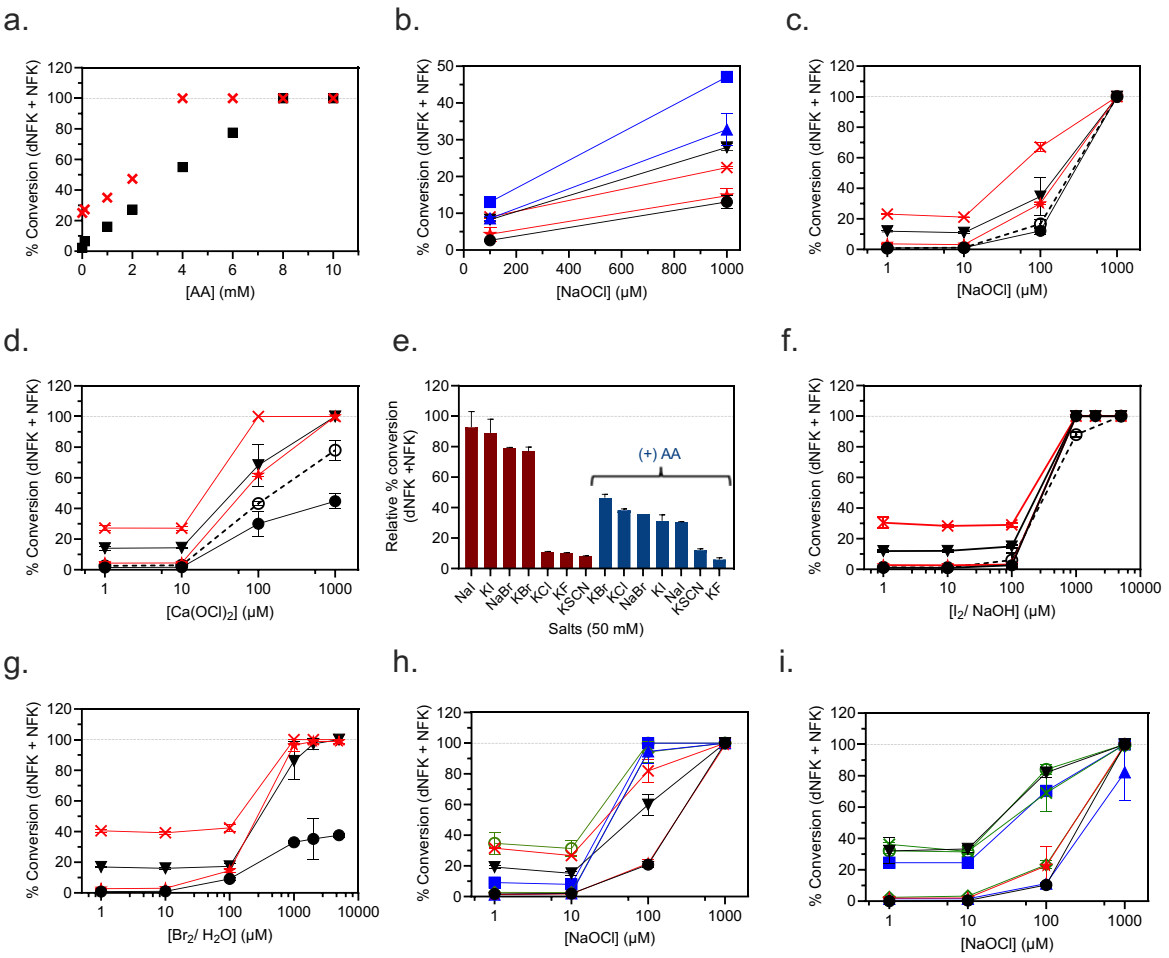

Figure 3. Characterization of recombinant human indoleamine 2,3-dioxygenase-1 (rhIDO1) with (pseudo)hypohalites. (a) Reactions with variable [ascorbic acid (AA)] and [NaOCl] = 100 mM (■) or 1 mM (✕). The dashed line represents 100% conversion of 1 mM L-Trp to products. (b) Reactions in the absence of AA and variable [NaOCl] without additional salts (**black** data points) after 2.5 h (●) and 18 h (▼); with 1 mM NaI (**red** data points) after 2.5 h (★) and 18 h (✕); or with 10 mM NaI (**blue** data points) after 2.5 h (▲) and 18 h (■). Note that trend lines are depicted and the y-axis scale is less than 100% conversion in order to better visualize the difference between the data points. (c) Semi-logarithmic plot for reactions with variable [NaOCl] with 5 mM AA after 2.5 h (●) and 18 h (▼) or with 10 mM AA after 2.5 h (★) and 18 h (✕); or reactions with 10 mM AA after 2.5 h (○) with rhIDO1 pre-treated with ferricyanide (dashed line). (d) Semi-logarithmic plot for reactions with variable [$Ca(OCl)_2$] with 5 mM AA after 2.5 h (●) and 18 h (▼) or with 10 mM AA after 2.5 h (★) and 18 h (✕); or reactions with 10 mM AA after 2.5 h (○) with rhIDO1 pre-treated with ferricyanide (dashed line). (e) Reactions using lactoperoxidase, H_2O_2, and indicated salt for the in situ generation of (pseudo)hypohalites, in the absence or presence of AA. (f) Semi-logarithmic plot for reactions with variable [I_2/ NaOH] with 5 mM AA after 2.5 h (●) and 18 h (▼) or with 10 mM AA after 2.5 h (★) and 18 h (✕); or reactions with 10 mM AA after 2.5 h (○) with rhIDO1 pre-treated with ferricyanide (dashed line). (g) Semi-logarithmic plot for reactions with variable [Br_2 (*aq*)] with 5 mM AA after 2.5 h (●) and 18 h (▼) or with 10 mM AA after 2.5 h (★) and 18 h (✕). (h) Semi-logarithmic plot for reactions

with variable [NaOCl] with 10 μM NaI after 2.5 h (●) and 18 h (▼); with 100 μM NaI after 2.5 h (★) and 18 h (✕); with 1 mM NaI after 2.5 h (▲) and 18 h (■); or with 10 mM NaI after 2.5 h (◇) and 18 h (○). (h) Semi-logarithmic plot for reactions with variable [NaOCl] with 10 μM NaBr after 2.5 h (●) and 18 h (▼); with 100 μM NaBr after 2.5 h (★) and 18 h (✕); with 1 mM NaBr after 2.5 h (▲) and 18 h (■); or with 10 mM NaBr after 2.5 h (◇) and 18 h (○).

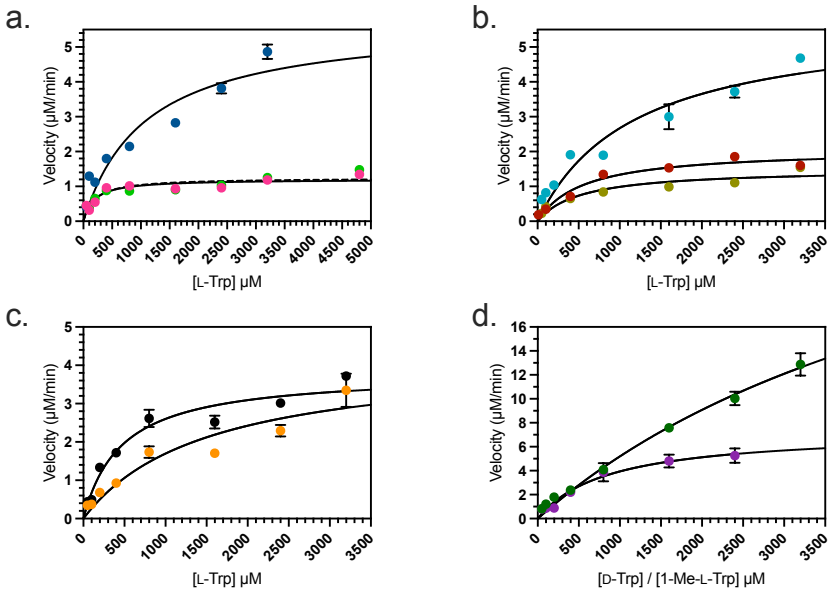

Figure 4. Michaelis-Menten plots for a single-substrate kinetic analysis of rhIDO1. rhIDO1 reactions with variable [L-Trp] and (a) 200 μM NaOCl (●), 1 mM NaOCl (●), and 200 μM NaOCl with 10 μg/mL catalase (●); (b) 100 μM $Ca(OCl)_2$ (●), 500 μM $Ca(OCl)_2$ (●), and 100 μM $Ca(OCl)_2$ and 100 μM NaBr (●); (c) 1 mM I_2/ NaOH (●), 1 mM Br_2/ H_2O (●); (d) with variable [D-Trp] and 100 μM $Ca(OCl)_2$ (●), and with variable [1-Me-L-Trp] and 200 μM NaOCl (●) .

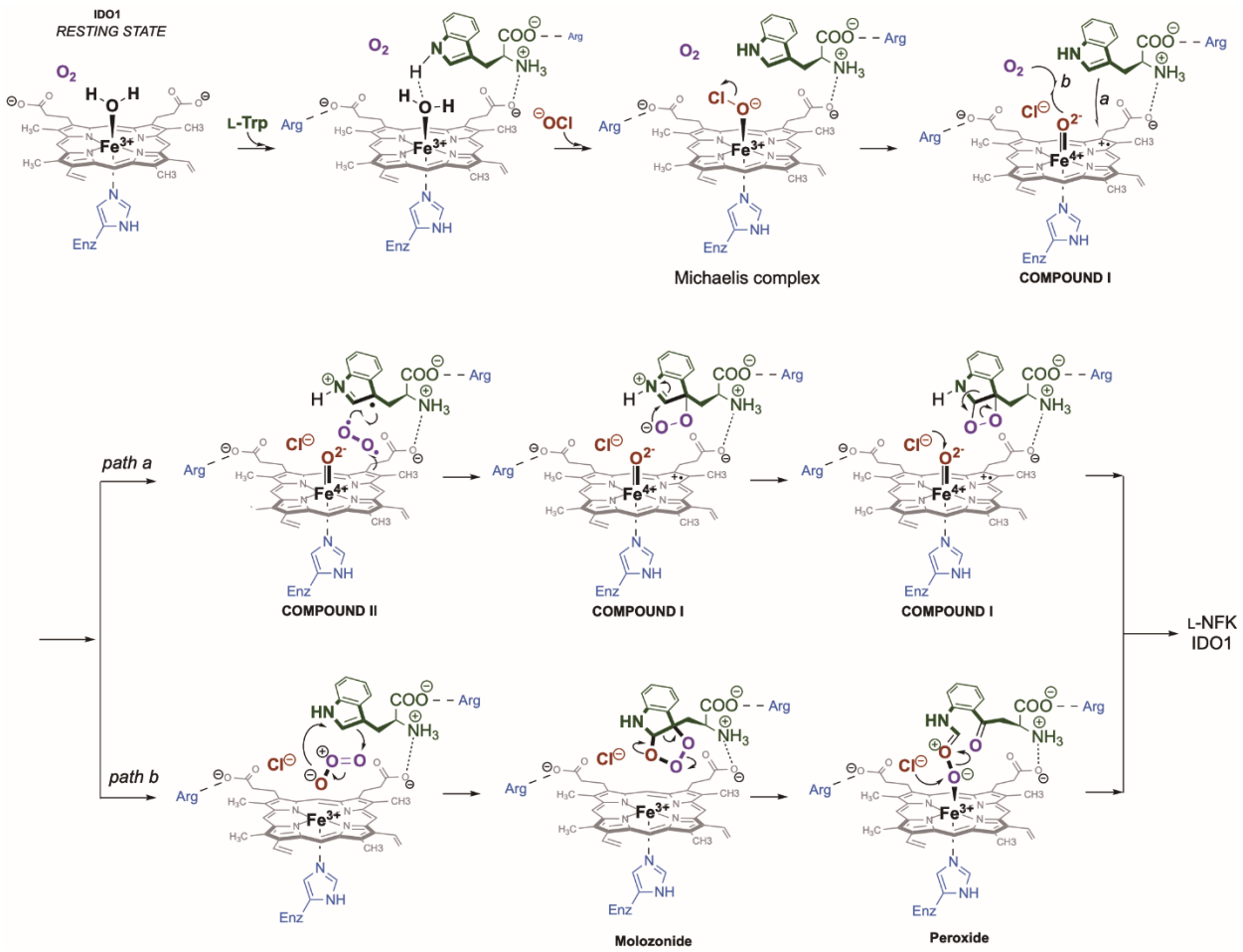

Figure 5: Hypothetical mechanism for rhIDO1-catalyzed conversion of L-Trp to L-NFK, with NaOCl as a catalytic cofactor/activator. The proposed binding interactions are based on several independent structures of rhIDO1, although protein dynamics likely alter these interactions during the catalytic cycle, which in turn is predicted to modulate the reducing power of the heme prosthetic group. The formation of Compound I mimics the peroxide shunt pathway that is realized with several hemoproteins. Compound I is proposed to proceed either through path a, forming a dioxetane intermediate or through path b, following an ozonolysis mechanism. In both routes, chloride is shown as the final reducing agent that regenerates heme-bound hypochlorite, thus behaving as a true cofactor. However, the possibility that the next cycle starts without regeneration of HOCl, hence behaving as a catalytic activator.